Shock-induced secondary vortices on a delta wing – An Euler simulation

Anand Kumar

CSIR Centre for Mathematical Modelling and Computer Simulation, Bangalore 560 037, India

Earlier Euler simulations of transonic flow over delta wings, in spite of using very fine grids, have not shown the shock-induced secondary vortices. It is shown here that this results from an inherent deficiency of the computational grids employed. By employing a grid that correctly takes into account the length scales of the flow, for the first time, a lee-side flow, containing embedded cross-flow shocks and shock-induced secondary vortices, is obtained, right from the apex of the wing.

TRANSONIC flow over delta wings is of interest to highly maneuverable fighter aircraft and missiles. On a sharp-edged delta wing the flow separates from the wing leading-edges forming the primary vortices. As the incidence is increased the outboard flow beneath the primary vortex can attain supersonic speeds. This flow, which is highly spanwise, must turn to align itself with the wind-side flow at the leading-edge. Under appropriate conditions, this may lead to the formation of a cross-flow shock, and a shock-induced secondary separation, leading to the formation of a secondary vortex.

Euler simulations of transonic vortex on sharp-edged delta wings have been carried out by several investigators. Hoeijmakers *et al.*[1] have presented results for a 65 deg wing employing O–O grid with over 1.2 million cells. Bannink and Houtman[2] have employed a 196,000 cells C–O grid, and a 270,000 cells H–O grid has been used by Hitzel[3] in their computations. Longo[4] has presented Euler results on a 70 deg delta wing for a range of incidence, employing a H–H grid consisting of 460,000 points. While some of these calculations have partially captured the cross-flow shock, the shock-induced secondary separation has not been obtained in any of the earlier computations.

The conventional grids cannot resolve the flow near the wing-apex due to dissimilar length scales of the flow and the grid[5]. As the apex is approached, the flow in the transverse plane scales with the local semi-span, whereas the transverse length scales of a conventional grid, for example H–O, C–O, O–O or H–H grid, do not. This inherent feature of conventional grids cannot be overcome by a simple grid refinement.

As will be shown here, the poorly-resolved near-apex flow, computed using a conventional grid, cannot capture the cross-flow shock, and hence the shock-induced secondary vortex. The vortex resolution improves as one moves away from the apex; but the poor resolution of the near-apex flow delays the shock formation. A fully resolved near-apex flow appears critical for the simulation of the shock-induced secondary vortex. This has been achieved here by employing an embedded conical (EC) grid[5] which correctly takes into account the length scales of the flow.

Experimental investigations[6,7] on 65 deg sharp-edged delta wings at M_∞ (free-stream Mach number) of 0.85 show that the secondary separation is shock-induced for α (angle of attack) of 15 deg and above. We present below the computed flow over a 65 deg sharp-edged delta wing of zero thickness at M_∞ of 0.85 and α of 15 deg. An EC grid having 294,212 cells (a 68 (chordwise) × 32 (wing-normal) × 64 (spanwise) inner conical grid with a 76 × 32 × 64 outer H–O grid), for the half-wing is employed. A comparable conventional H–O grid having 311,296 cells (76 × 64 × 64) is also employed. The Euler method and the grid generation method are described in ref. 5.

Figure 1 shows the EC solution C_p contours in the first transverse cell plane (TCP) downstream of the

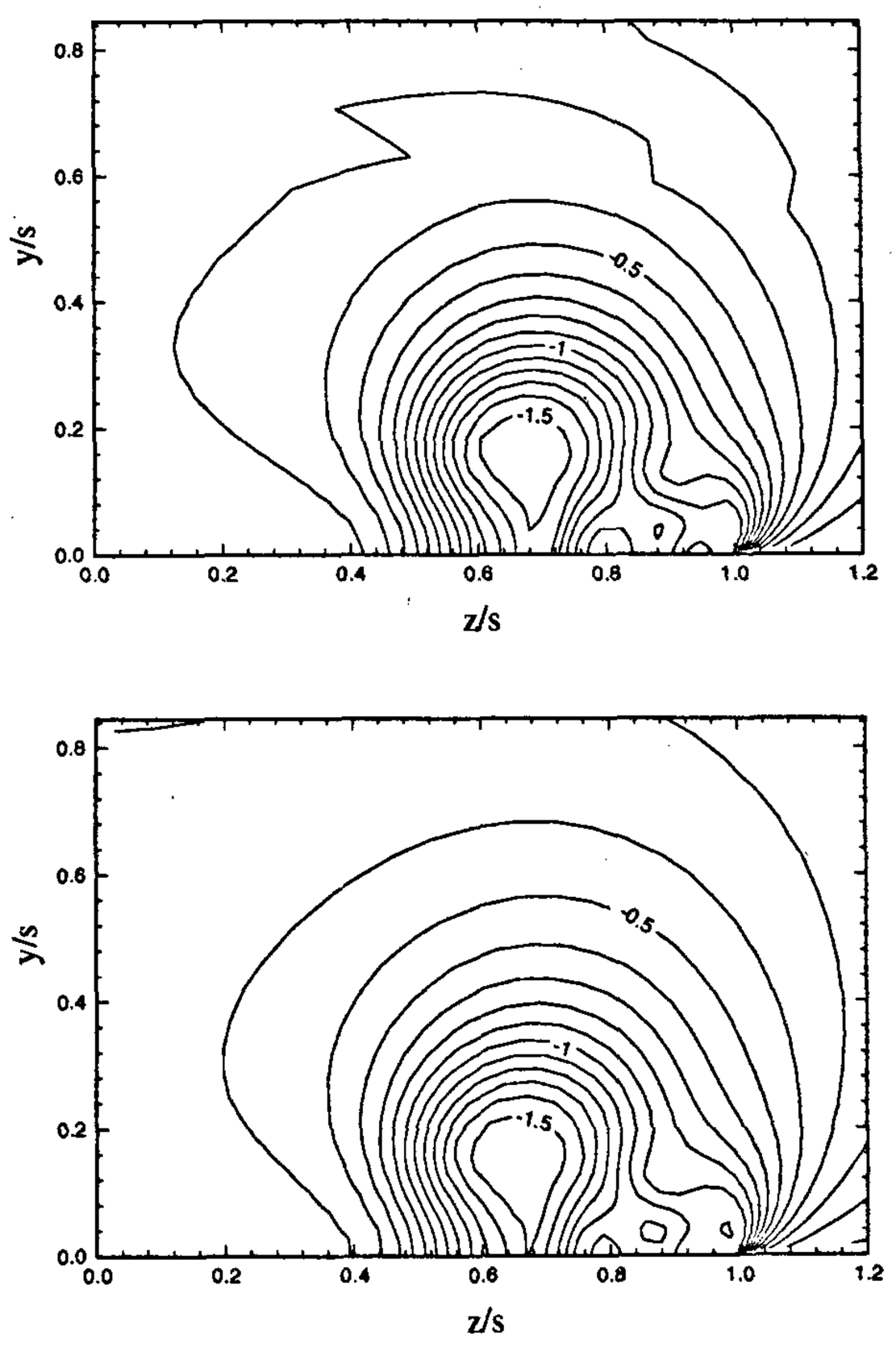

Figure 1. Contours of C_p at $x = 0.00128$ (1st TCP), and at $x = 0.3048$ (19th TCP).

apex, which is at $x=0.00128$ (x, y, and z are the coordinates along the root-chord, wing-normal and span-wise directions, with the origin located at the wing-apex, and linear dimensions are scaled by the root-chord), and at $x=0.3048$ (19th TCP). The vortex is seen to be fully resolved right from the first TCP. Further, the similarity of the plots in the two TCPs indicates the nearly conical nature of the flow in the fore part of wing. A cross-flow shock, located on the lee-surface at about $z/s=0.72$ (s is the local semi-span), can be seen from the contours. The secondary vortex core can also be seen from the C_p contours.

A shock wave can occur only when M_b, the Mach number component normal to local isobaric surface, exceeds one[8]. Figure 2 *a* shows contours of M_b in the first TCP, with the C_p contours superimposed over it. We see that just ahead of the cross-flow shock, the value of M_b is more than one. Figure 2 *b* shows the conically projected velocity vectors in the first TCP, along with a few streamlines through this vector field. Downstream of the cross-flow shock, the near surface streamlines moves away from the surface, leading to the formation of the secondary vortex. We thus see that the present EC grid computation is able to capture the experimentally observed shock-induced secondary vortex, right from the apex.

In comparison, Figure 3 shows the H–O solution C_p contours at $x=0.02158$ (5th TCP) and at $x=0.3048$ (19th TCP). The vortex structure is seen to be poorly formed even in the 5th TCP, which is due to fewer grid points in the wing-normal direction to resolve the flow. The poorly formed vortex generates a lower suction in the vortex core and on the lee-surface. Due to the poorly-formed pressure and velocity fields, M_b does not exceed one in the 5th TCP, and hence a cross-flow shock cannot occur near the apex. However, as one moves away from the apex, the vortex becomes better

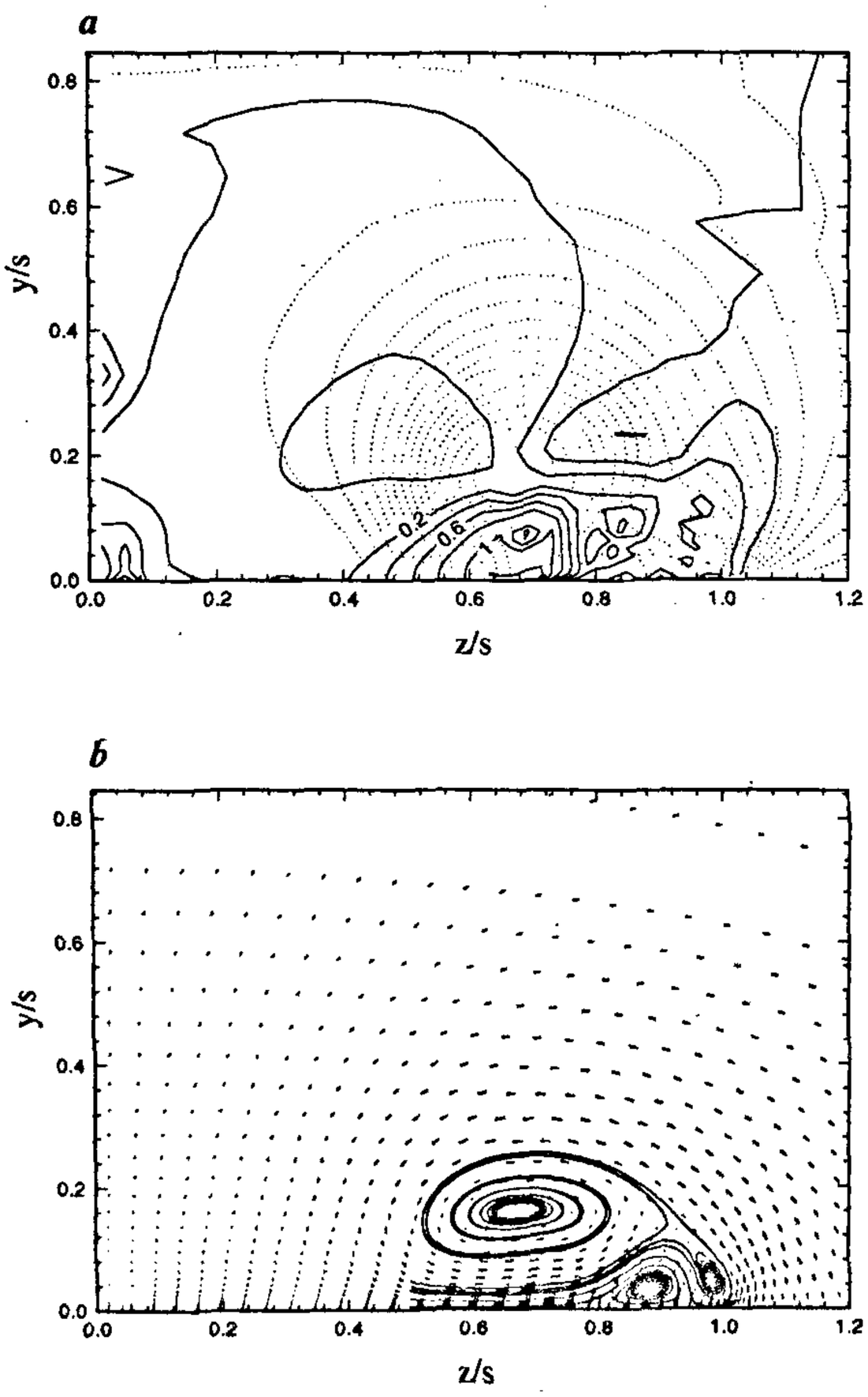

Figure 2. *a*, Contours of M_b along with C_p contours (dotted), and *b*, conically projected velocity vectors along with some streamlines, in the 1st TCP.

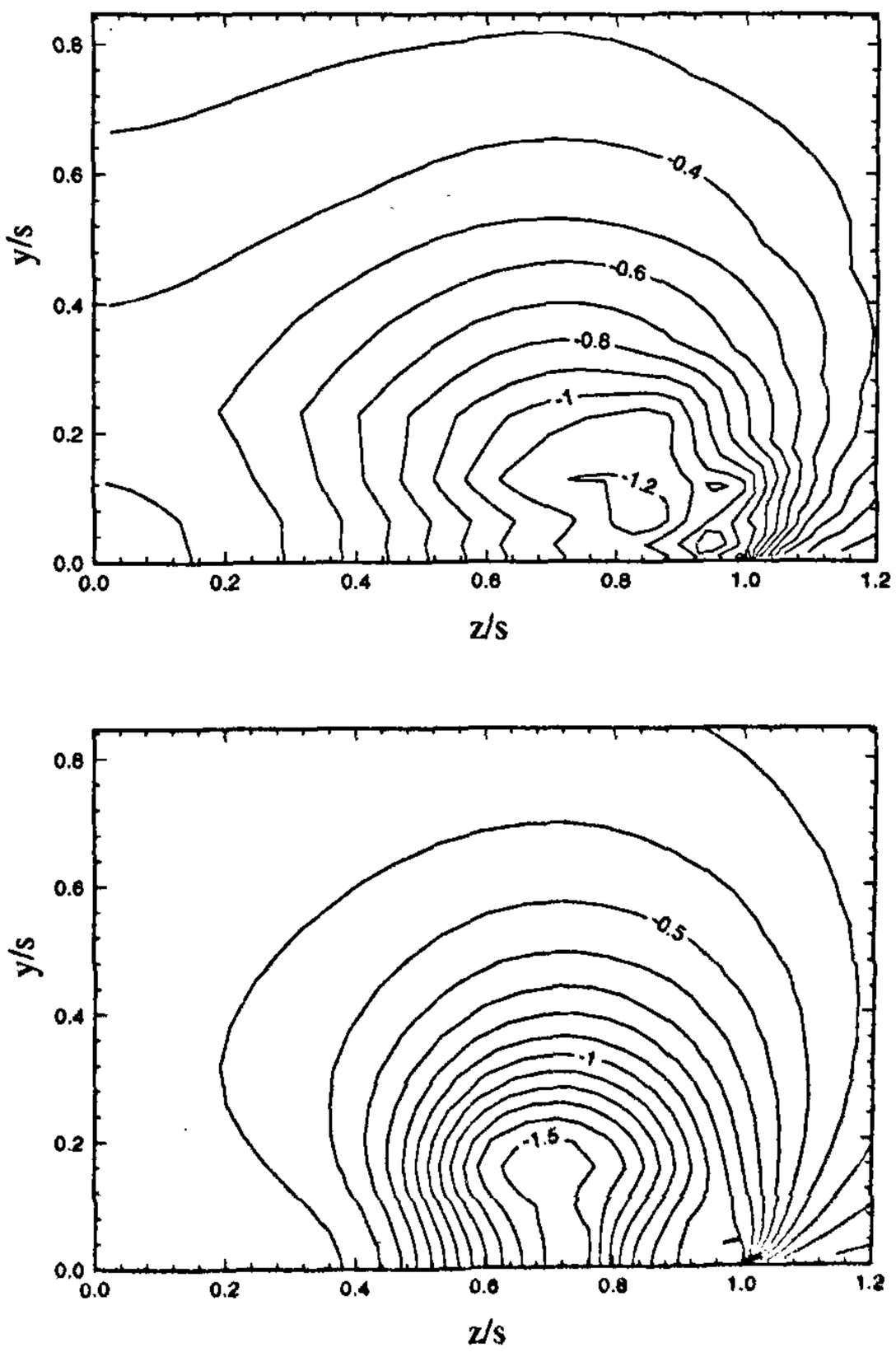

Figure 3. H–O solution C_p contours at $x=0.02158$ (5th TCP), and at $x=0.3048$ (19th TCP).

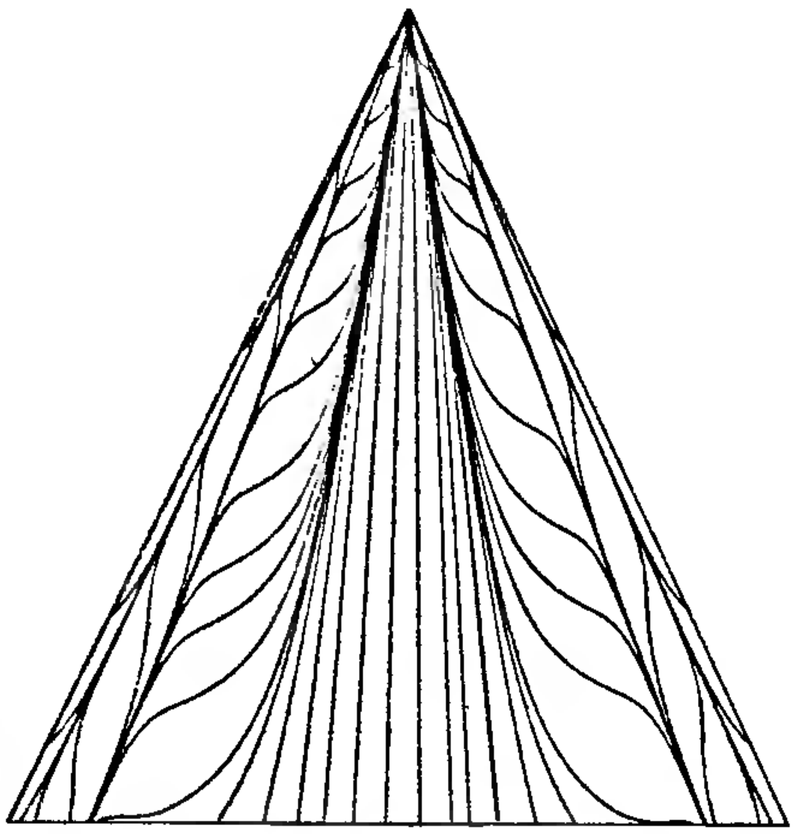

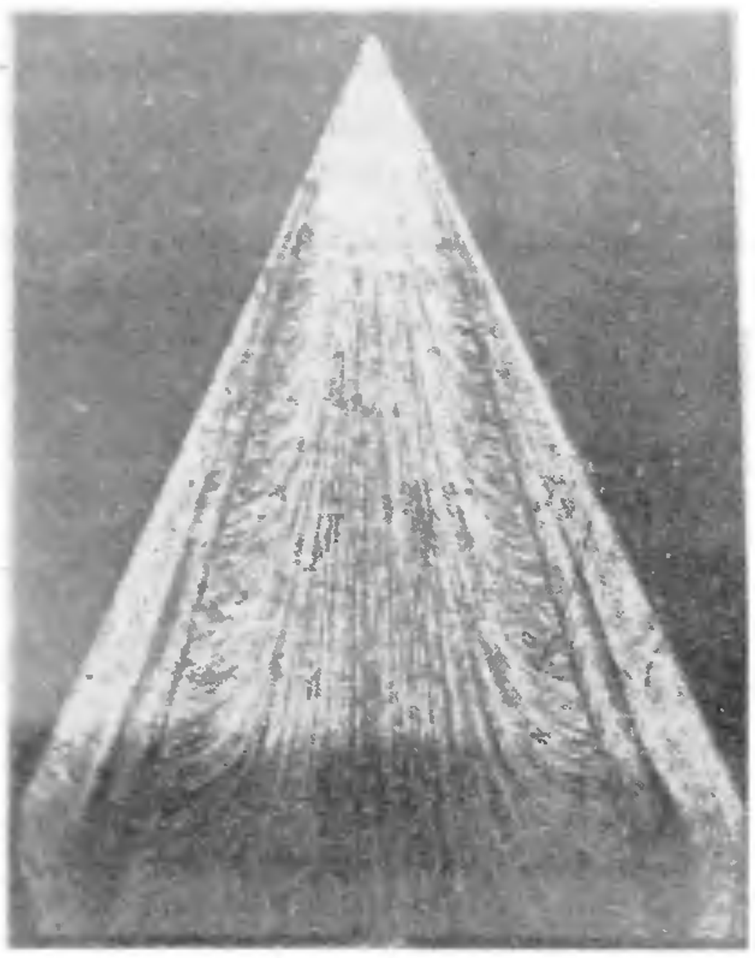

Figure 4. Computed and experimental lee-surface flow.

formed, as can be seen from the C_p contours in the 19th TCP. Compared to that in the 5th TCP, the suction in the vortex core in the 19th TCP is higher, and the C_p contours are just beginning to cluster immediately outboard of the foot of the vortex, indicating that a weak shock may be forming.

Figure 4 shows the lee-surface flow pattern given by the EC solution, and the experimental surface oil-flow visualization[2]. The computed near-conical surface-flow pattern is similar to that observed in the experiment, although it may be noted that the boundary layer in the experiment can modify the velocity vector orientation. A sharp change in the direction of the oil streak-lines and the computed surface streamlines near the secondary separation show the cross-flow shock. The cross-flow shock is seen to terminate the conically outboard flow and give rise to the secondary separation.

We have shown that an accurate simulation of the near-apex flow is necessary for the simulation of the cross-flow shock and, hence, the shock-induced secondary separation. By employing a grid, namely an embedded conical grid, that correctly takes into account the length scales of the flow considered, we have been able to capture, for the first time, the experimentally observed transonic vortex structure with embedded cross-flow shock and the shock-induced secondary vortex, right from the apex of the wing.

1. Hoeijmakers, H. W. M., Jacobs, J. M. J. W. and Van Den Berg, J. I., in Proceedings of the 17th International Council of the Aeronautical Sciences, 1990, vol. 1, pp. 486–499.
2. Bannink, W. J. and Houtman, E. M., in *IUTAM Symposium on Fluid Dynamics of High Angles of Attack* (eds Kawamura, R. and Aihara, Y.), Springer, Berlin, 1993, pp. 399–411.
3. Hitzel, S. M., 'Wing vortex flows up into vortex breakdown – A numerical simulation', AIAA Paper 88-2518, 1988.
4. Longo, J. M., *Am. Inst. Aeronaut. Astronaut. J.*, 1995, **33**, 680–687.
5. Kumar, A., *Am. Inst. Aeronaut. Astronaut. J.*, 1996, **34**, 2038–46.
6. Houtman, E. M. and Bannink, W. J., 'Experimental investigation of the transonic flow at the leeward side of a delta wing at high incidence', Report LR-518, TU Delft, 1987.
7. Elsenaar, A. and Hoeijmakers, H. W., 'An experimental study of the flow over a sharp-edged delta wing at subsonic and transonic speeds', AGARD CP-494, Paper No. 15, 1990.
8. Bickley, W. G., 'Critical conditions for compressible flow', ARC R&M No. 2330, 1950.

Received 4 April 1997; accepted 2 May 1997

Plasmid profile of *Erwinia herbicola* ATCC 21998

S. Koul, V. Verma, Anand Kumar* and G. N. Qazi

Division of Biotechnology, Regional Research Laboratory (CSIR), Canal Road, Jammu Tawi 180 001, India
*School of Biotechnology, Devi Ahilya University, Khandwa Road, Indore 452 001, India

Extra-chromosomal genome study of *Erwinia herbicola* ATCC 21998 was carried out. Two plasmids (pVQ1, pVQ2: mol. wt 7.4 and 8.0 kb respectively) were identified. One of the plasmids (pVQ2) was cured off and a restriction endonuclease map of the other plasmid (pVQ1) is established. *E. herbicola* ATCC 21998 being a keto-acid producing bacteria like *Gluconobacter oxydans* ATCC 9937 converts glucose to 2,5-diketo gluconic acid by a membrane-bound direct